Endocrine (2019) 65:426–439
https://doi.org/10.1007/s12020-019-01952-7

ORIGINAL ARTICLE

Check for updates

Mir-494 inhibits osteoblast differentiation by regulating BMP signaling in simulated microgravity

WeiWei Qin[1,2] · Li Liu[1] · YongChun Wang[3] · Zhe Wang[4] · AnGang Yang[5] · Tao Wang[6]

Received: 27 February 2019 / Accepted: 5 May 2019 / Published online: 25 May 2019

Abstract

Although the BMPR-SMAD-RUNX2 signaling pathway plays widely recognized roles in BMP-induced osteogenesis, factors regulating this pathway remain to be defined. In this study, we used simulated microgravity models, which represent mechanical unloading conditions, to detect miRNAs that function in osteoblast differentiation. We found that miR-494 was persistently increased in C2C12 cells subjected to clinorotation conditions and in osteoblasts isolated from tail-suspended rats. Experiments showed that the overexpression of miR-494 correlated with a marked reduction in osteoblast differentiation genes and a decrease in osteogenesis in BMP2-induced osteogenetic differentiation. In contrast, the inhibition of miR-494 promoted BMP2-induced osteogenesis and partially rescued osteoblast differentiation disorder under simulated microgravity conditions. Mechanism studies revealed that miR-494 directly targeted BMPR2 and RUNX2, both of which play vital roles in the BMPR-SMAD-RUNX2 signaling pathway. More importantly, we demonstrated a positive feedback loop between miR-494 and MYOD, a critical transcription factor for myogenesis, indicating that miR-494 may participate in deciding cell fate of the multipotent mesenchymal stem cells (MSCs). Collectively, our study reveals an important role for miR-494 in regulating osteogenesis, the identification of which not only clarifies a regulator of BMP2-induced osteoblast differentiation, but also offers a possible strategy for preventing bone loss under microgravity conditions.

Keywords Osteogenesis · Osteoblast differentiation · miRNA · BMP2 · Simulated microgravity

Introduction

Osteoblast differentiation is a critical step in the maintenance of bone homeostasis and is generally maintained by growth hormone and various other endocrine and autocrine/paracrine factors. Multiple signaling pathways, including BMP, Wnt, and Notch, play important roles in osteoblast differentiation [1]. BMP2 is one of the most potent osteoblast differentiation factors in vitro, and signaling through BMP2 is transduced from the plasma membrane receptors to the nucleus mainly through the BMPR-SMAD-RUNX2 pathway [2]. Although the BMPR-SMAD-RUNX2 signaling pathway is one of the best-defined osteogenesis pathways, additional factors, including miRNAs, that regulate BMP2 signaling remain to be identified.

miRNAs are small regulatory RNAs that serve important roles in a variety of diverse physiological and pathological processes, including cell proliferation, apoptosis, cancer,

These authors contributed equally: WeiWei Qin, Li Liu

Supplementary information The online version of this article (https://doi.org/10.1007/s12020-019-01952-7) contains supplementary material, which is available to authorized users.

✉ AnGang Yang
agyang@fmmu.edu.cn

✉ Tao Wang
wangt@fmmu.edu.cn

[1] Department of Hematology, Tangdu Hospital, Fourth Military Medical University, 710038 Xi'an, China

[2] State Key Laboratory of Cancer Biology, Department of Biochemistry and Molecular Biology, Fourth Military Medical University, 710032 Xi'an, China

[3] Department of Aerospace Biodynamics, School of Aerospace Medicine, Fourth Military Medical University, 710032 Xi'an, China

[4] Department of Nuclear Medicine, Xijing Hospital, Fourth Military Medical University, 710032 Xi'an, China

[5] Department of Immunology, Fourth Military Medical University, 710032 Xi'an, China

[6] Department of Medical Genetics and Developmental Biology, Fourth Military Medical University, 710032 Xi'an, China

and metabolic abnormalities [3–6]. Recent evidence has shown that osteogenetic induction and differentiation are also regulated by miRNAs [7–11]. Mouse studies in which mature miRNA production was ablated by the conditional deletion of Dicer alleles at different stages of bone formation have demonstrated that miRNAs control early and late steps of osteogenesis [7]. Huang J. et al. also reported that miR-204 and miR-211 act as important endogenous negative regulators of RUNX2. The expression of these miRNAs results in the inhibition of osteogenesis and an increase in adipogenesis in mesenchymal progenitor cells and bone marrow stem cells [12]. Furthermore, RUNX2 negatively regulates the miRNA cluster miR-23a–27a–24-2 by a feed-forward mechanism that causes the derepression of SATB2 and RUNX2, suggesting an important role of this miRNA cluster in the progression and maintenance of the osteocyte phenotype [13]. Moreover, miR-125 [14], miR-133, and miR-135 [15] inhibit the differentiation of osteoprogenitors in ST2 and C2C12 mesenchymal cells, whereas miR-29b [16] and miR-2861 [17] have been characterized as positive regulators of osteoprogenitor differentiation by targeting inhibitors of osteoblast differentiation. However, most of the aforementioned studies on osteoblast differentiation were conducted under conditions of normal gravity and mechanical loading. The function of miRNAs in osteoblast differentiation under microgravity or unloading conditions remains largely unknown.

In this study, we used microarrays to determine the miRNA expression profiles in C2C12 cells under simulated microgravity conditions. Our results show a marked increase in miR-494 expression when C2C12 cells were exposed to simulate microgravity conditions. Furthermore, miR-494 inhibits osteogenesis by direct inhibiting two pivotal factors of the BMP signaling, BMPR2 and RUNX2. We also experimentally determined that miR-494 was under the control of the key myogenic transcription factor MYOD. Consistent with the importance of miR-494 under simulated microgravity conditions, the inhibition of miR-494 expression partially rescued the defects in osteoblast differentiation under simulated microgravity conditions.

Materials and methods

Cell culture

Mouse pre-myogenic C2C12 cells and HEK 293T cells were purchased from the Classical Type Collection (Shanghai, China) and were maintained in Dulbecco's Modified Eagle Medium (DMEM; Life Technologies, Grand Island, NY, USA) containing 10% FBS (Life Technologies, Grand Island, NY, USA) and antibiotics (100 U/ml of penicillin-G and 100 µg/ml of streptomycin) at 37 °C in a humidified atmosphere in the presence of 5% CO_2. Osteogenesis was induced by following a previously published protocol [18]. Briefly, cells were cultured in medium containing 0.25% BSA for 24 h, after which they were treated with 300 ng/ml recombinant human BMP2 (R&D Systems, Minneapolis, MN, USA) or vehicle (as control) and harvested at the indicated time points.

Statistical analysis

Statistical analysis was performed using SPSS 15.0 software (SPSS Inc., USA). Data are expressed as the mean ± standard deviation from at least three separate experiments. Differences between groups were analyzed using Student's *t*-test to compare two groups or by one-way ANOVA for the comparison of more than two groups. A *p*-value of $P < 0.05$ was considered to be statistically significant.

More detailed "Materials and methods" are available in the Supplemental section.

Results

Osteogenesis is suppressed under simulated microgravity conditions

To identify the alterations in osteoblast differentiation induced by microgravity at the cellular level, multipotent mesenchymal progenitor C2C12 cells were cultured under clinorotation conditions for 72 h, and then quintessential osteoblast differentiation markers, including alkaline phosphatase (ALP), osteocalcin (OC), osterix (OSX), and runt-related transcription factor 2 (RUNX2), were monitored by qRT-PCR. All of these genes were downregulated (Fig. 1a), which is consistent with previous reports [19, 20]. Next, we used a tail-suspended rat model, which mimics a simulated microgravity environment by suspending the load from the hind limbs of the rat to evaluate the in vivo osteogenetic effects of microgravity. Bone formation and loss in the rats were monitored by radionuclide bone scintigraphy at different time points after the initiation of tail suspension. Compared with the control group, tail-suspended rats showed greater than 30% decrease in the accumulation of ^{99m}Tc-MDP in the bones and the joints by the end of the second week of tail suspension. Bone loss was even more obvious after a 4-week tail-suspension, at which point bone formation decreased by approximately 50% compared with the control rats (Fig. 1b). These results suggest that osteoblast differentiation and bone formation are suppressed under simulated microgravity conditions.

To evaluate the effects of BMP2 on osteoblast differentiation under simulated microgravity conditions, C2C12 cells were treated with 300 ng/ml BMP2 under normal

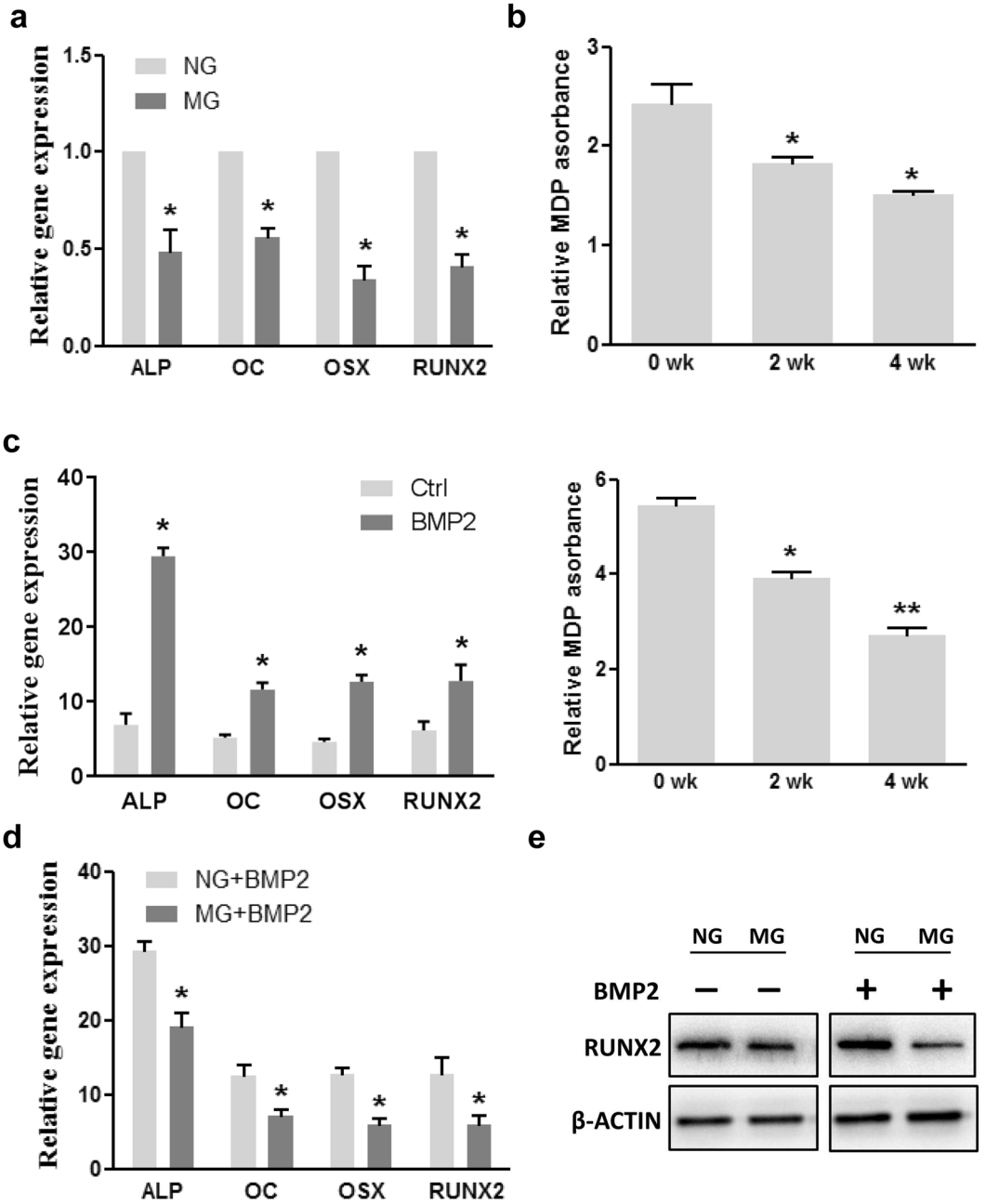

Fig. 1 Osteoblast differentiation and maturation are suppressed under simulated microgravity conditions. **a** C2C12 cells were cultured with clinorotation for 72 h and then harvested for subsequent analysis. qRT-PCR was performed to determine the expression of several osteogenesis genes. ALP alkaline phosphatase, OC osteocalcin, OSX osteoprotegerin, RUNX2 runt-related transcription factor 2, NG normal gravity, and MG simulated microgravity. **b** The tail-suspended hind limb unloading rat model was performed as described in the "Materials and methods" section. Bone scintigraphy images were taken at the indicated time points, and ^{99m}Tc-MDP accumulation was calculated to determine bone metabolic activity in the bones (upper) and joints (lower). **c** C2C12 cells were cultured for 72 h in the presence of 300 ng/ml BMP2 or vehicle control, after which qRT-PCR analysis was performed. **d** C2C12 cells were cultured for 72 h in the presence of 300 ng/ml BMP2 under normal gravity and simulated microgravity culture conditions. Cells were then harvested and qRT-PCR analysis was performed. **e** Western blot analysis of cell lysates obtained from C2C12 cells treated without (−) or with (+) 300 ng/ml BMP2 under normal gravity and simulated microgravity culture conditions. GAPDH was used to normalize the qRT-PCR data. Data shown represent the mean ± SD based on three independent experiments. $^{*}p < 0.05$, $^{**}p < 0.01$

culture conditions and clinorotation culture conditions. As expected, osteoblast differentiation markers significantly increased when BMP2 was added to the culture medium (Fig. 1c). However, BMP2-induced C2C12 osteoblast differentiation was circumvented when cells were cultured under simulated microgravity conditions (Fig. 1d). Similar

results were also observed in MC3T3-E1 pre-osteoblast cells (data not shown). We then determined the protein expression levels of RUNX2, the key transcriptional factor in osteoblast differentiation, in BMP2-treated C2C12 cells under normal gravity and simulated microgravity conditions. Our results revealed that although RUNX2 expression increased in BMP2-treated cells compared with the untreated control cells, the RUNX2 protein levels decreased under simulated microgravity conditions compared with cells cultured under normal gravity in the presence and absence of BMP2 (Fig. 1e), indicating that the inhibition of osteogenesis occurs under simulated microgravity conditions, even in the presence of BMP2.

miR-494 is upregulated in response to simulated microgravity conditions

Because miRNAs play important roles in a variety of physiological and pathological processes, we investigated whether miRNAs might also contribute to the inhibition of osteoblast differentiation under simulated microgravity conditions. C2C12 cells were cultured under normal conditions and under clinorotation for 12 h, after which microarrays were performed to detect changes in miRNA expression during early time points of exposure to simulate microgravity conditions. Of the hundreds of miRNAs analyzed, miR-494 showed a twofold increase, whereas miR-18*, miR-122a, miR-143, miR-301, and miR-340 showed decreases in expression greater than twofold (Fig. 2a). Next, qPCR was performed to verify the results from the microarray. Consistent with the microarray data, miR-494 showed robust upregulation, whereas miR-340 and miR-122a showed significant downregulation in C2C12 cells when cultured under clinorotation conditions. However, in contrast with the microarray results, significant changes were not observed for the expression of miR-18*, miR-143, and miR-301 (Fig. 2b). Next, we validated the expression pattern of miR-494, miR-122a, and miR-301 during osteoblast differentiation in C2C12 cells under simulated microgravity conditions at different time. C2C12 cells were cultured under clinorotation conditions for 0, 2, 8, 12, 24, 48, and 72 h, after which the cells were harvested and prepared for qPCR analysis. miR-494 expression increased immediately after simulated weightlessness, and although there was a slight decrease in miR-494 expression at the 24 h time point, the increase in miR-494 expression persisted until the end of the 3-day observation period, reaching levels of expression sixfold greater than baseline expression (Fig. 2c). In contrast, miR-340 and miR-122a showed persistently decreased levels, with ~70% reduction in miR-340 expression and 90% reduction in miR-122a expression after 72 h of clinorotation (Fig. 2c).

To further evaluate the expression patterns of these miRNAs in osteoblasts over a longer time period in an in vivo setting, we performed qPCR using osteoblasts isolated from tail-suspended rats. Consistent with the results from the clinorotation cell experiment, our results showed that miR-494 expression markedly increased after 2 weeks of tail-suspension by almost tenfold and further increased to approximately 30-fold after 4 weeks of tail suspension (Fig. 2d). However, we found no obvious expression changes for either miR-340 or miR-122a after 2 or 4 weeks of tail suspension (Fig. 2d); this is in contrast with our in vitro data, in which C2C12 cells showed consistently decreased miR-340 and miR-122a expression (Fig. 2c). These results indicate that in osteoblasts, miR-494, miR-340, and miR-122a are gravity-sensitive miRNAs. However, the decrease in miR-340 and miR-122a expression caused by simulated weightlessness can be compensated in a longer time, whereas the increase in miR-494 expression could not be compensated under simulated microgravity conditions and increases rapidly in a time-dependent manner. Considering that simulated microgravity induces osteoporosis and bone loss [21–23], we speculated that miR-494 might play a role in osteoblast differentiation and abnomal simulated microgravity-induced osteblastogenesis.

miR-494 inhibits the BMP2-induced differentiation of osteoblasts in vitro

To study the effect of miR-494 expression on osteoblasts, we transfected miR-494 mimics and miR-494 inhibitors into C2C12 cells. Cell proliferation levels were measured by the MTT assay, which revealed that neither miR-494 mimics nor miR-494 inhibitor had significant effects on cell proliferation in either cell line (Fig. S1). Next, we assessed the rate of osteoblast differentiation in C2C12 cells transfected with miR-494 mimics in the presence of 300 ng/ml BMP2. qPCR results revealed that ectopic expression of miR-494 decreased the mRNA levels of ALP, OC, OSX, and RUNX2 in C2C12 cells (Fig. 3a). Notably, although BMP2 stimulated osteoblast differentiation, miR-494 expression markedly inhibited the capacity of BMP2 to upregulate osteoblast markers in cells (Fig. 3a).

In addition to the changes in the mRNA levels of these osteoblast genes, we performed enzyme assays, histological staining, ELISA, and western blotting to evaluate changes in the protein levels of these markers as well as changes in their functional capacity. ALP activity in C2C12 cells transfected with miR-494 was significantly decreased relative to cells transfected with negative control (NC) in the presence and absence of BMP2 (Fig. 3b). The downregulation of ALP activity was further confirmed by histological staining (Fig. 3c). Similar results were observed for RUNX2. RUNX2 protein expression was upregulated in the presence of BMP2, but was decreased in cells transfected with miR-494 compared with cells transfected with NC

a

miRNA	Fold change (MG/NG)
Upregulated （>2）	
No_known_mmu_target	2.045201266
mmu-miR-494	2.000001825
Downregulated (<0.5)	
mmu-miR-301	0.477787174
mmu-miR-143	0.494417542
mmu-miR-340	0.496169601
mmu-miR-18a*	0.49880401
mmu-miR-122	0.499452011

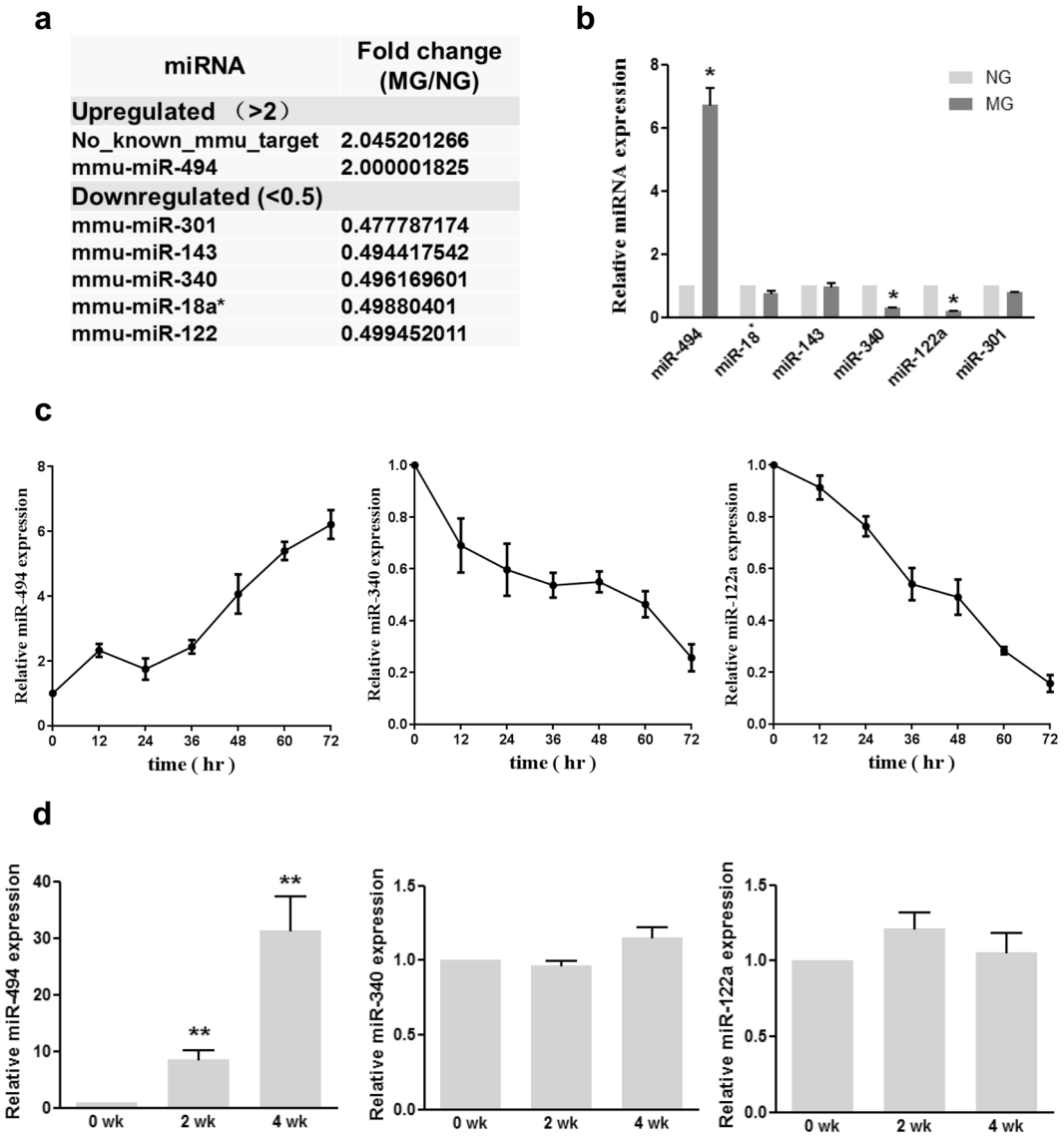

Fig. 2 miR-494 was downregulated under simulated microgravity conditions. **a** miRNA microarray analysis of C2C12 cells cultured under normal gravity or simulated microgravity culture conditions for 12 h. miRNAs with a fold-change (MG versus NG) > 2 or <0.5 are shown. **b** qRT-PCR analysis of selected miRNAs that were differentially regulated in the cells as described in (**a**). **c** qRT-PCR analysis of miR-494, miR-340, and miR-122a in C2C12 cells under simulated microgravity culture conditions at the indicated time points. **d** qRT-PCR analysis of miR-494, miR-340, and miR-122a in osteoblasts isolated from tail-suspended rats at the indicated time points. The mouse U6 gene was used to normalize the qRT-PCR data. Data shown represent the mean ± SD based on three independent experiments. $*p < 0.05$, $**p < 0.01$

(Fig. 3d). Moreover, ELISA analysis showed that miR-494 reduced the secretion of OC induced by BMP2 (Fig. 3e). These data suggest that miR-494 can inhibit osteoblast differentiation induced by BMP2.

Because mesenchymal stem cells have multipotent differentiation potential, we determined whether miR-494 might play roles in myogenesis and adipogenesis. To this end, we used qPCR to examine the expression of key genes involved in myogenesis and adipogenesis in miR-494-transfected C2C12 cells. We found that ectopic expression of miR-494 increased the expression level of the myogenic genes MYOD and MYOGENIN, whereas the reduction of endogenous miR-494 correlated with decreased expression of MYOD and MYOGENIN (Fig. 3f, g). The expression of PPARγ, a transcription factor involved in adipose differentiation, was not affected by the introduction of miR-494 (Fig. 3h). Taken together, our data suggest that miR-494 not only inhibits osteoblastic differentiation in C2C12 cells but also promotes muscle-specific differentiation.

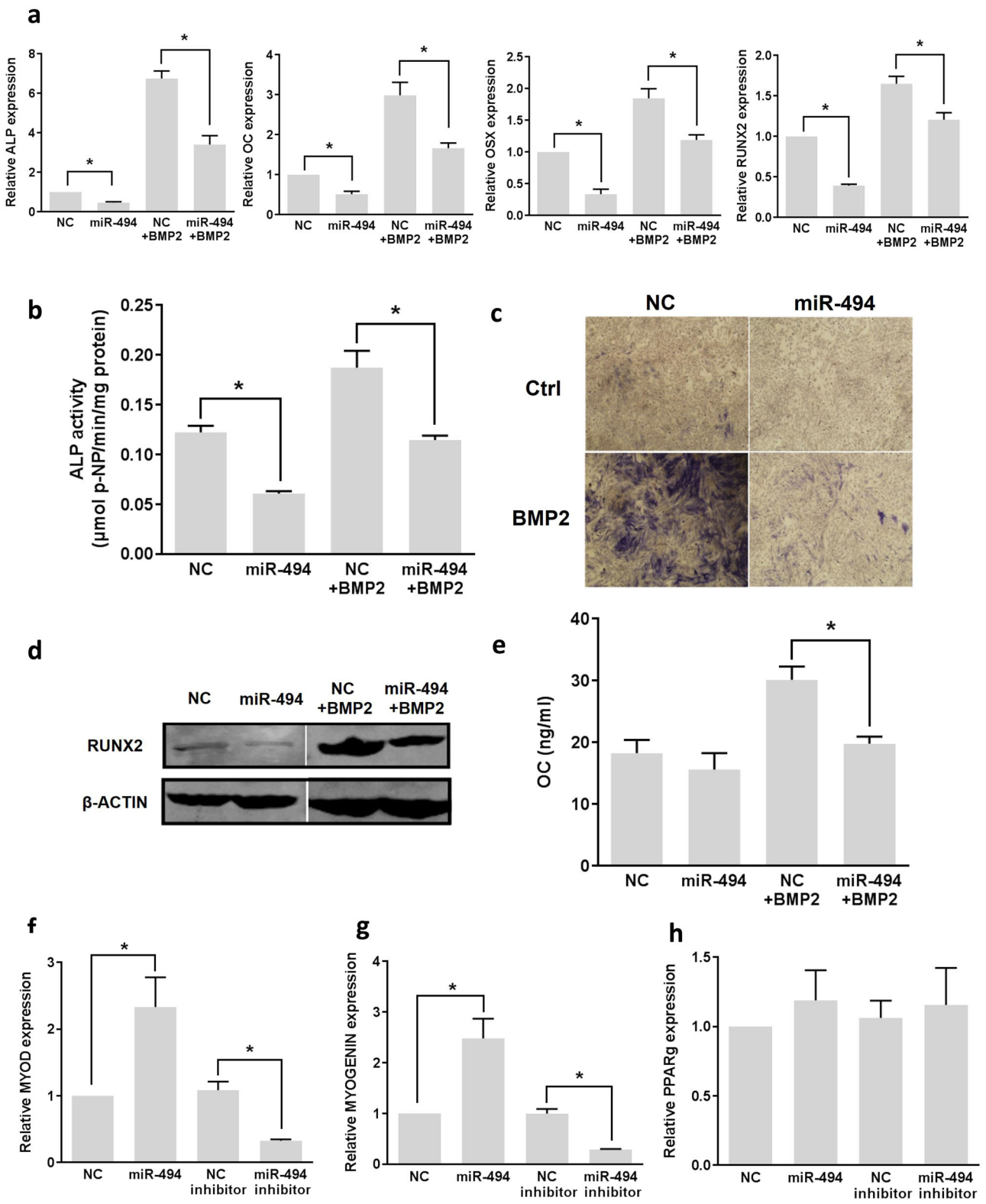
a
Relative ALP expression
Relative OC expression
Relative OSX expression
Relative RUNX2 expression
NC
miR-494
NC +BMP2
miR-494 +BMP2
b
ALP activity (μmol p-NP/min/mg protein)
c
NC
miR-494
Ctrl
BMP2
d
RUNX2
β-ACTIN
e
OC (ng/ml)
f
Relative MYOD expression
NC inhibitor
miR-494 inhibitor
g
Relative MYOGENIN expression
h
Relative PPARg expression

◀ **Fig. 3** miR-494 inhibits BMP2-induced differentiation of osteoblasts in vitro. **a**–**f** C2C12 cells transfected with miR-494 or negative control (NC) were treated with or without 300 ng/ml BMP2 for 72 h. After treatment, qRT-PCR analysis was performed to detect changes in the mRNA levels of ALP, OC, OSX, and RUNX2 (**a**). ALP activity (**b**) and ALP histological staining (**c**) were analyzed to determine the functional level and total protein level of ALP. Western blot and ELISA were conducted to detect protein changes of RUNX2 (**d**) and OC (**e**). **g**–**i** C2C12 cells were transfected with NC, miR-494, NC miRNA inhibitor, or miR-494 inhibitor for 72 h, after which the cells were harvested. qRT-PCR analysis was performed to detect changes in the mRNA levels of MYOD (**g**), MYOGENIN (**h**) and PPARγ (**i**). GAPDH was used to normalize the qRT-PCR data. Data shown represent the mean ± SD based on three independent experiments. $*p < 0.05$, $**p < 0.01$

BMPR2 and RUNX2 are direct targets of miR-494 in C2C12 cells

To understand the mechanism by which miR-494 inhibits osteoblast differentiation, we sought to determine the specific targets of miR-494 that are relevant to bone formation. Using TargetScan, Pictar, and miRBase programs and databases, we searched for potential miR-494 targets. Over 1000 genes with at least one binding site corresponding to the mature miR-494 sequence were identified as candidates (data not shown). From the predicted genes, we selected 18 putative miR-494 target genes, all of which are cell cycle regulators, transcription factors or signaling molecules involved in osteogenesis. All of the 3′-untranslated region (3′-UTR) sequences containing putative miR-494 binding sites of the selected genes were cloned into a pGL3-based luciferase reporter vector and were co-transfected with miR-494 or NC into 293A cells (Fig. S2). miR-494 cotransfection markedly reduced the luciferase activity in cells transfected with reporter plasmids containing BMPR2 and RUNX2 compared with NC, indicating that these genes could be legitimate targets of miR-494 (Fig. S2). We then made several mutations within the seed regions of the miR-494 binding sites of the reporter plasmids, after which luciferase reporter assays were performed in 293A cells. We found no clear change in the luciferase signal in cells transfected with the mutated reporter plasmids relative to cells that received the NC control, suggesting that suppression of the luciferase activity is specific to miR-494 (Fig. 4b). Additional experiments showed that when C2C12 cells were transfected with miR-494, the mRNA and protein levels of BMPR2 and RUNX2 decreased significantly (Fig. 4c, d). Taken together, our data suggest that BMPR2 and RUNX2 are novel miR-494 target genes.

miR-494 inhibits BMP2-induced osteogenesis through BMPR2 and RUNX2

To further address whether miR-494 prevented osteogenesis by targeting BMPR2 and RUNX2, we used siRNA constructs to silence these three genes in C2C12 cells. When C2C12 cells were transfected with the siRNA constructs, the expression of BMPR2 and RUNX2 decreased significantly (Fig. 5a). qPCR analysis suggested that knockdown of BMPR2 and RUNX2 in C2C12 cells resulted in the suppression of osteoblast differentiation markers (ALP, OC, OSX, and RUNX2). Similarly, when miR-494 or mixed siRNA constructs targeting BMPR2 and RUNX2 were transfected into cells, BMP2-induced osteogenesis was equally suppressed (Fig. 5b).

To test whether miR-494 inhibits BMP2-induced osteogenesis through BMPR2 and RUNX2, we performed a "rescue" experiment in which BMPR2 and RUNX2 were reintroduced by an expression plasmid containing the BMPR2 or RUNX2 coding sequence into miR-494-transfected and BMP2-treated C2C12 cells. We found that the simultaneous ectopic expression of miR-494 and the BMPR2 or RUNX2 coding sequence rescued the inhibitory effect of miR-494 on osteoblast differentiation (Fig. 5c). These results indicate that miR-494 suppresses BMP2-induced C2C12 osteogenetic differentiation by inhibiting BMPR2 and RUNX2 expression.

miR-494 inhibitor partially rescues the functional defects of osteoblasts cultured in the presence of simulated microgravity

Based on our results suggesting that miR-494 inhibits osteogenesis, we expected the knockdown of miR-494 to have the opposite effect on osteoblast differentiation under simulated microgravity conditions. C2C12 cells were transfected with either miR-494 inhibitor or inhibitor control and then were cultured under clinorotation conditions for 72 h before harvest. qPCR was performed to monitor the expression of osteogenetic markers. Our results show that in the presence of 300 ng/ml BMP2, which induces osteoblast differentiation, miR-494 inhibitor significantly increased the expression of ALP, OC, OSX, and RUNX2 compared with the control inhibitor, suggesting that miR-494 inhibition promotes osteogenesis under simulated microgravity conditions (Fig. 6a). However, in the non-BMP2-treated group, compared with the inhibitor control, miR-494 inhibitor showed no obvious change in osteogenetic marker expression (Fig. 6a). In addition, the ability of miR-494 inhibitor to partially rescue simulated microgravity-induced osteogenetic differentiation suppression was further demonstrated using an ALP staining assay, the results of which showed stronger ALP staining in the miR-494 inhibitor-treated group compared with the control-treated group (Fig. 6b). Finally, we observed a significant increase in the BMPR2 and RUNX2 expression level in C2C12 cells subjected to clinorotation when miR-494 inhibitor was added regardless of the presence or absence of BMP2 (Fig. 6c, d). Altogether, our data show that knocking

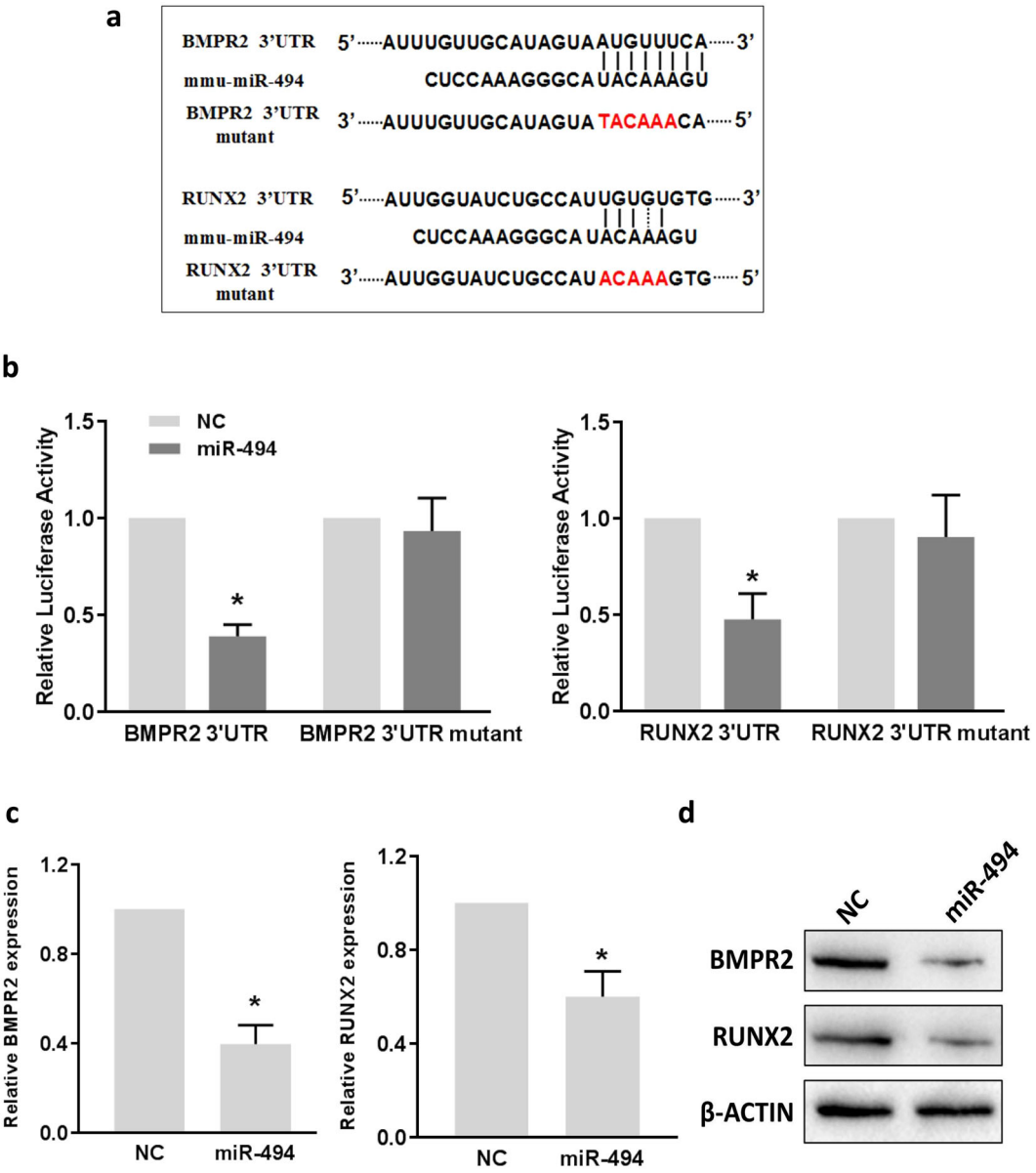

Fig. 4 miR-494 targets BMPR2 and RUNX2 in C2C12 cells. **a** The predicted wild-type miR-494 binding sequences within the 3′-UTR of BMPR2 and RUNX2 and mutated derivatives of these binding sites. **b** pGL3 constructs containing wild-type or mutated 3′-UTR sequences corresponding to BMPR2 or RUNX2 were cotransfected into cells along with scrambled miRNA or miR-494 mimics. Luciferase activity was measured 48 h after transfection. **c**, **d** C2C12 cells transfected with miR-494 mimics or control oligonucleotides were subjected to qRT-PCR (**c**) or western blot analysis (**d**). GAPDH was used to normalize the qRT-PCR data. Data shown represent the mean ± SD based on three independent experiments. $*p < 0.05$, $**p < 0.01$

down endogenous miR-494 could partially rescue simulated microgravity-induced osteoblast differentiation defects and thus could be used to understand and prevent osteoporosis in spaceflight.

Myogenic transcription factor MYOD positively regulates the expression of miR-494

The functional identification of the regulatory genes upstream of miRNAs that are responsible for controlling the spatial and temporal expression of specific miRNAs is vital for a comprehensive understanding of the functions of miRNAs. We examined possible transcription factors that might be involved in the regulation of miR-494 by using the TRANSFAC online database. We noticed the presence of several predicted MYOD binding sites within the 3-kb upstream region of mouse pre-mir-494. A MYOD/MYOG binding site (−40) and a MYOD/E47 binding site (−166) were predicted in the proximal portion of this region, a MYOD/E47 binding site (−908) was found in the middle of

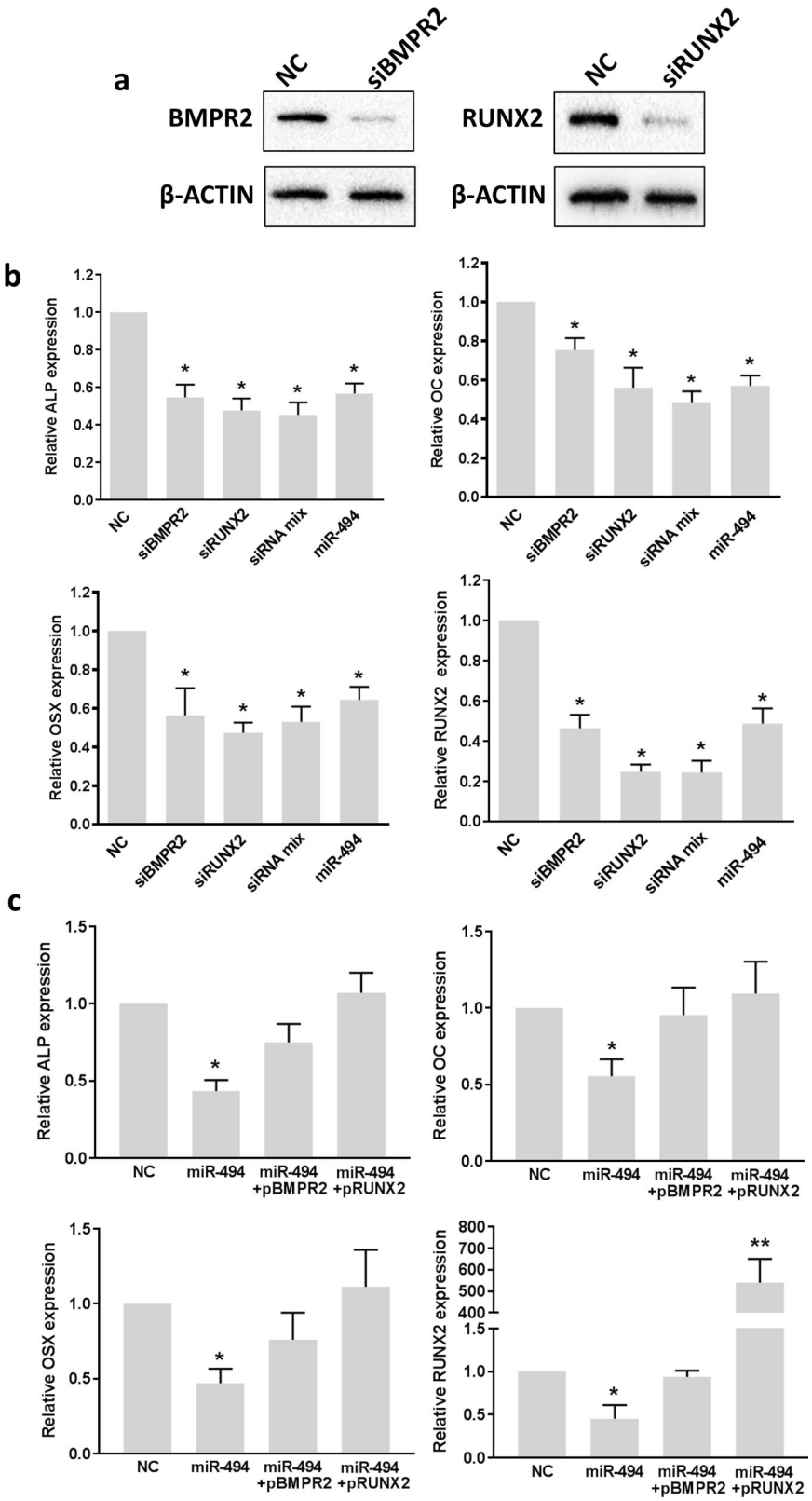

Fig. 5 miR-494 inhibits BMP2-induced osteogenesis through RUNX2 and BMPR2. **a** C2C12 cells were transfected with siRNA or negative control siRNA for 48 h. Western blot analysis of BMPR2 and RUNX2 was conducted to determine the knockdown efficiency of the siRNA constructs. **b** C2C12 cells were transfected with siRNA, negative control siRNA, or miR-494 for 12 h, at which point BMP2 was added to the culture medium at a final concentration of 300 ng/ml. Cells were cultured for an additional 72 h before harvesting the cells and subjecting them to qRT-PCR analysis. **c** C2C12 cells were transfected with negative control and miR-494 with or without BMPR2 expression plasmid and RUNX2 expression plasmid in combination with miR-494 for 12 h, at which point BMP2 was added to the culture medium at a final concentration of 300 ng/ml. Cells were cultured for an additional 72 h before harvesting the cells and subjecting them to qRT-PCR analysis. GAPDH was used to normalize the qRT-PCR data. Data shown represent the mean ± SD based on three independent experiments. $^{*}p < 0.05$, $^{**}p < 0.01$

this region, and a MYOD binding site (−2700) was observed in the distal portion of this region (Fig. 7a). Based on the function of MYOD as a key transcription factor in regulating muscle differentiation and based on the mutual exclusivity of muscle differentiation and osteogenesis differentiation, we investigated whether MYOD might play a

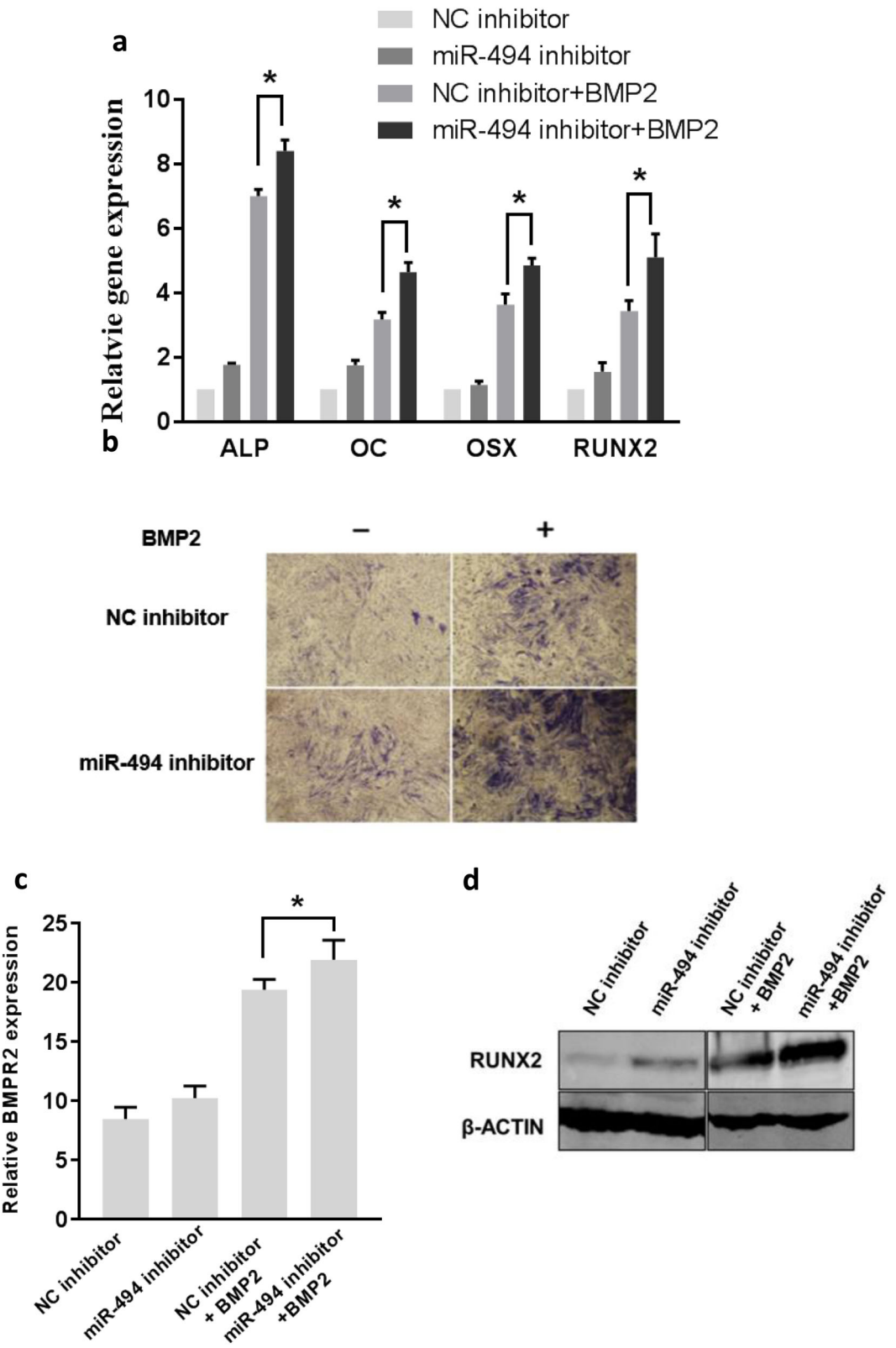

Fig. 6 miR-494 partially rescues simulated microgravity-induced osteoblast differentiation defects. C2C12 cells were transfected with miR-494 or negative control miRNA and were cultured in the presence or absence of 300 ng/ml BMP2 under clinorotation conditions for 72 h. Then, the cells were harvested and subjected to qRT-PCR (**a**, **c**), ALP histological staining (**b**), and western blotting (**d**) analyses

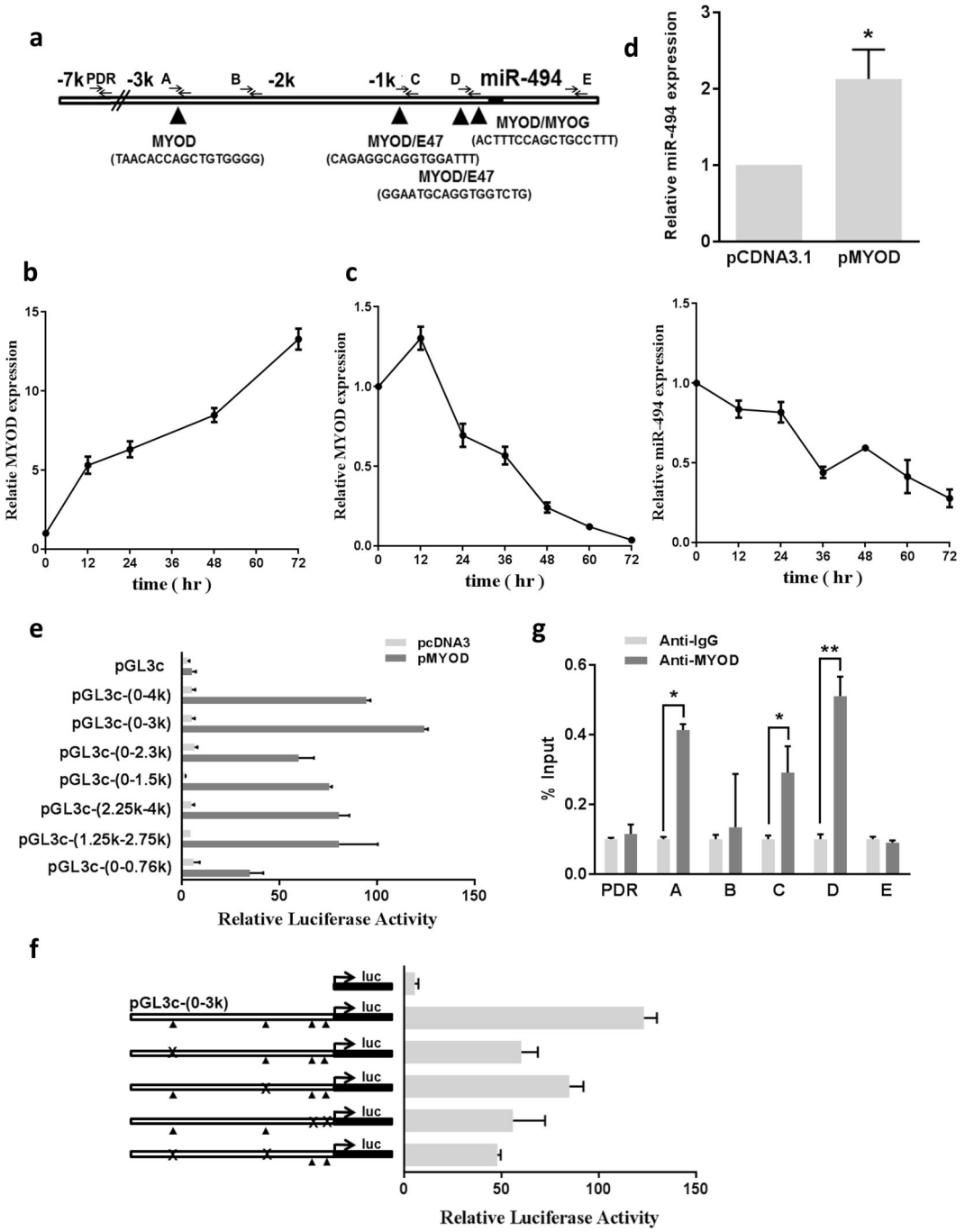

Fig. 7 miR-494 is regulated by the myogenic transcription factor MYOD. **a** Schematic diagram of the mouse miR-494 gene and its upstream regulatory region illustrating the MYOD binding sites and the primers used for ChIP analysis. **b** C2C12 cells cultured under simulated microgravity conditions were harvested at the indicated time points, and qRT-PCR analysis was performed. **c** C2C12 cells were treated with 300 ng/ml BMP2 and then were harvested at the indicated time points and analyzed by qRT-PCR. **d** C2C12 cells were transfected with pCDNA3.1 or pMYOD for 48 h, after which the cells were analyzed by qRT-PCR. **e** Reporter plasmids containing different lengths of the miR-494 upstream regulatory region were cotransfected with either pCDNA3.1 or pMYOD into C2C12 cells for 48 h, after which luciferase activity was determined. **f** Luciferase assay results from C2C12 cells cotransfected with pMYOD and different reporter plasmids containing 3 kb of sequence upstream of miR-494 but lacking the proximal, middle or distal MYOD binding sites. **g** ChIP analysis results from C2C12 cells using anti-MYOD antibody to probe for enrichment in miR-494 gene and miR-494 regulatory sequence pull-down relative to nonspecific IgG (control). Quantitative PCR was used to determine the fold-enrichment of MYOD-miR-494 binding. PDR: primers for a "promoter desert" region of genomic DNA upstream of the miR-494 promoter. GAPDH was used to normalize the qRT-PCR data. Data shown represent the mean ± SD based on three independent experiments. $*p < 0.05$

role in regulating miR-494 expression. To address this hypothesis, we analyzed MYOD expression in clinorotated C2C12 cells and found that MYOD mRNA increased in a time-dependent manner (Fig. 7b). In contrast, during BMP2-induced osteogenesis differentiation in C2C12 cells, MYOD expression gradually decreased, which correlated perfectly with the decrease in miR-494 expression (Fig. 7c). To determine whether MYOD regulates the expression of miR-494, we transfected C2C12 cells with pMYOD, which expresses the MYOD coding sequence in the pcDNA3.1 vector backbone. We detected a greater than twofold increase in miR-494 expression 48 h after the transfection, indicating a positive regulatory relationship between MYOD and miR-494 expression (Fig. 7d).

Next, we explored whether the regulation of miR-494 by MYOD occurred via the direct binding of MYOD in the regulatory region of miR-494 by using a luciferase reporter system. We constructed several reporter plasmids by introducing different lengths of upstream DNA sequence into the pGL3-control vector. The results of the luciferase assay in C2C12 cells showed that transfection of the control vector pcDNA3.1 did not affect the luciferase activity level in the presence of any of the constructs; however, transfection of pMYOD caused a significant increase in luciferase activity (Fig. 7e). pMYOD transfection increased luciferase expression more than 100-fold in the presence of the pGL3c-(0–3k) and pGL3c-(0–4k) constructs, both of which contain all four predicted MYOD binding sites. In other constructs that lack one, two or three MYOD binding sites, luciferase expression increased 30- and 80-fold, respectively, suggesting that the proximal, middle and distal MYOD binding sites functional and important in the regulation of miR-494 transcription (Fig. 7e). We also constructed several reporter plasmids in which the proximal, middle or distal MYOD binding sites were mutated. These plasmids were cotransfected with pMYOD vector into C2C12 cells, and luciferase activity was measured 48 h post transfection. Consistent with the results of the truncated luciferase reporter assay, the results of the mutated sites suggest that all MYOD binding sites upstream of miR-494 play important roles in regulating miR-494 expression (Fig. 7f). Finally, chromatin immunoprecipitation assays were performed, which revealed that the proximal, middle, and distal MYOD binding sites were bound directly by MYOD (Fig. 7g). Taken together, our data show that the myogenic transcription factor MYOD can bind to the upstream regulatory region of miR-494 to positively regulate miR-494 transcription.

Discussion

In normal bone, equilibrium exists between bone formation and resorption. Systemic hormones and local factors regulate bone remodeling that involves the resorption of bone by osteoclasts and the deposition and mineralization of bone matrix by osteoblasts [24, 25]. Biomechanical forces play critical roles in the development of the skeletal system [26–29], whereas mechanical unloading or microgravity, which is encountered during spaceflight or confined bed rest, can cause bone loss and osteoporosis [20, 23, 30, 31]. Microgravity-induced osteoporosis is one of the main problems associated with spaceflight and has been estimated to cause a decrease of ~2% in bone mineral density after only 1 month [20, 23]. Although the molecular mechanism remains unclear, studies have indicated that the microgravity-induced changes in bone mass are associated with decreased bone formation and increased bone resorption [19, 32–34].

miRNAs play diverse roles in different physiological and pathological processes, including osteogenesis [7, 8, 12, 13, 15]. However, the involvement and the mechanism underlying changes in miRNA expression and their target genes involved in osteogenesis regulation under microgravity conditions remain poorly understood. Using a well-defined cell model that simulates weightlessness, we analyzed the miRNA expression profile in C2C12 cells and found that miR-494 was markedly increased under simulated microgravity conditions. We tested the function of miR-494 in BMP2-induced osteogenetic differentiation and demonstrated its suppressive role in this process (Fig. 3). Importantly, inhibition of miR-494 could partially rescue the functional defect of osteoblasts in simulated microgravity (Fig. 6), indicating that miR-494 might be a potential target for preventing bone loss and osteoporosis during spaceflight.

miR-494 is located within the Dlk1-Dio3 imprinted locus on human chromosome 14q32, a region that contains 54 miRNAs and constitutes one of the largest miRNA clusters in the human genome [35]. Several studies have explored the expression patterns and the clinical significance of this vital genomic region given that miRNA clusters play important roles in development and disease, including cancer [36–38]. However, the expression pattern and roles of miR-494 in different types of tumors remain controversial, suggesting that miR-494 may exhibit tissue-dependent expression and context-dependent function [39–43].

In a report that identified 11 miRNAs involved in pathological pathways activated in skeletal muscle damage and regeneration by the absence of dystrophin and by acute ischemia, miR-494 was upregulated in human myoblasts following differentiation [44]. miR-494 was characterized as one of the “regeneration miRNAs” that is induced in MDX mice, patients with DMD, the regenerative phase of the hind-limb ischemia response, and newborn mice, indicating a potent role for miR-494 in the promotion of skeletal muscle differentiation and regeneration [44]. Intriguingly,

our study describes another crucial function of miR-494 in restraining the differentiation of multipotent mesenchymal progenitor C2C12 cells toward osteogenesis. miR-494 regulates BMP signaling by directly targeting BMPR2 and RUNX2, and thus suppresses BMP2-induced osteogenetic differentiation at multiple levels. Importantly, we identified that miR-494 is controlled by the myogenic transcription factor MYOD, which is consistent with our observation that miR-494 facilitates myoblastic lineage differentiation while inhibiting osteogenetic differentiation. More interestingly, we noticed that ectopic expression of miR-494 upregulated the myogenic markers MYOD and MYOGENIN in C2C12 cells, indicating a positive feedback loop between MYOD and miR-494 that synergistically promotes myogenic differentiation (Fig. 3f, g). Collectively, our findings suggest that miR-494 plays a pivotal role in bone formation by negatively regulating osteogenetic differentiation. However, the molecular mechanisms through which miR-494 promotes myoblast differentiation and whether miR-494 also plays a role in adipose differentiation will require further exploration.

Funding This study was funded by the National Natural Science Foundation of China (81773003, 81472633, and 81400110).

Compliance with ethical standards

Conflict of interest The authors declare that they have no conflict of interest.

Ethical approval All animal experiments complied with ethical regulations were approved by the Medical Ethics Committee of FMMU. This article does not contain any studies with human participants performed by any of the authors.

Publisher's note: Springer Nature remains neutral with regard to jurisdictional claims in published maps and institutional affiliations.

References

1. G.L. Lin, K.D. Hankenson, Integration of BMP, Wnt, and notch signaling pathways in osteoblast differentiation. J. Cell. Biochem. **112**, 3491–3501 (2011). https://doi.org/10.1002/jcb.23287
2. V. Rosen, BMP2 signaling in bone development and repair. Cytokine growth factor Rev. **20**, 475–480 (2009). https://doi.org/10.1016/j.cytogfr.2009.10.018
3. V. Ambros, The functions of animal microRNAs. Nature **431**, 350–355 (2004). https://doi.org/10.1038/nature02871
4. P.D. Zamore, B. Haley, Ribo-gnome: the big world of small RNAs. Science **309**, 1519–1524 (2005). https://doi.org/10.1126/science.1111444
5. R. Visone, C.M. Croce, MiRNAs and cancer. Am. J. Pathol. **174**, 1131–1138 (2009). https://doi.org/10.2353/ajpath.2009.080794
6. V. Rottiers, A.M. Naar, MicroRNAs in metabolism and metabolic disorders. Nat. Rev. Mol. Cell Biol. **13**, 239–250 (2012). https://doi.org/10.1038/nrm3313
7. T. Gaur et al. Dicer inactivation in osteoprogenitor cells compromises fetal survival and bone formation, while excision in differentiated osteoblasts increases bone mass in the adult mouse. Dev. Biol. **340**, 10–21 (2010). https://doi.org/10.1016/j.ydbio.2010.01.008
8. J.B. Lian et al. MicroRNA control of bone formation and homeostasis. Nat. Rev. Endocrinol. **8**, 212–227 (2012). https://doi.org/10.1038/nrendo.2011.234
9. Y.X. Sun et al. MicroRNA-144-3p inhibits bone formation in distraction osteogenesis through targeting Connexin 43. Oncotarget **8**, 89913–89922 (2017). https://doi.org/10.18632/oncotarget.20984
10. S.R. Sera, N.I. Zur Nieden, microRNA regulation of skeletal development. Curr. Osteoporos. Rep. **15**, 353–366 (2017). https://doi.org/10.1007/s11914-017-0379-7
11. C. Wang, H. Liao, Z. Cao, Role of osterix and MicroRNAs in bone formation and tooth development. Med Sci. Monit. **22**, 2934–2942 (2016)
12. J. Huang, L. Zhao, L. Xing, D. Chen, MicroRNA-204 regulates Runx2 protein expression and mesenchymal progenitor cell differentiation. Stem Cells **28**, 357–364 (2010). https://doi.org/10.1002/stem.288
13. Hassan, M.Q. et al. A network connecting Runx2, SATB2, and the miR-23a~27a~24-2 cluster regulates the osteoblast differentiation program. Proc. Natl Acad. Sci. USA **107**, 19879–19884, (2010) https://doi.org/10.1073/pnas.1007698107.
14. Y. Mizuno et al. miR-125b inhibits osteoblastic differentiation by down-regulation of cell proliferation. Biochem. Biophys. Res. Commun. **368**, 267–272 (2008). https://doi.org/10.1016/j.bbrc.2008.01.073
15. Li, Z. et al. A microRNA signature for a BMP2-induced osteoblast lineage commitment program. Proc. Natl Acad. Sci. USA **105**, 13906–13911, (2008) https://doi.org/10.1073/pnas.0804438105.
16. Z. Li et al. Biological functions of miR-29b contribute to positive regulation of osteoblast differentiation. J. Biol. Chem. **284**, 15676–15684 (2009). https://doi.org/10.1074/jbc.M809787200
17. H. Li et al. A novel microRNA targeting HDAC5 regulates osteoblast differentiation in mice and contributes to primary osteoporosis in humans. J. Clin. Investig. **119**, 3666–3677 (2009). https://doi.org/10.1172/JCI39832
18. E. Balint et al. Phenotype discovery by gene expression profiling: mapping of biological processes linked to BMP-2-mediated osteoblast differentiation. J. Cell. Biochem. **89**, 401–426 (2003). https://doi.org/10.1002/jcb.10515
19. M. Zayzafoon, W.E. Gathings, J.M. McDonald, Modeled microgravity inhibits osteogenic differentiation of human mesenchymal stem cells and increases adipogenesis. Endocrinology **145**, 2421–2432 (2004). https://doi.org/10.1210/en.2003-1156
20. M. Zayzafoon, V.E. Meyers, J.M. McDonald, Microgravity: the immune response and bone. Immunol. Rev. **208**, 267–280 (2005). https://doi.org/10.1111/j.0105-2896.2005.00330.x
21. J.D. Sibonga, Spaceflight-induced bone loss: is there an osteoporosis risk? Curr. Osteoporos. Rep. **11**, 92–98 (2013). https://doi.org/10.1007/s11914-013-0136-5
22. T.P. Stein, Weight, muscle and bone loss during space flight: another perspective. Eur. J. Appl. Physiol. **113**, 2171–2181 (2013). https://doi.org/10.1007/s00421-012-2548-9
23. J. Klein-Nulend, R.G. Bacabac, J.P. Veldhuijzen, J.J. Van Loon, Microgravity and bone cell mechanosensitivity. Adv. Space Res **32**, 1551–1559 (2003). https://doi.org/10.1016/S0273-1177(03)90395-4
24. L.J. Raggatt, N.C. Partridge, Cellular and molecular mechanisms of bone remodeling. J. Biol. Chem. **285**, 25103–25108 (2010). https://doi.org/10.1074/jbc.R109.041087
25. T. Martin, J.H. Gooi, N.A. Sims, Molecular mechanisms in coupling of bone formation to resorption. Crit. Rev. Eukaryot. Gene Expr. **19**, 73–88 (2009)

26. J. Klein-Nulend, R.G. Bacabac, A.D. Bakker, Mechanical loading and how it affects bone cells: the role of the osteocyte cytoskeleton in maintaining our skeleton. Eur. Cells Mater. **24**, 278–291 (2012)
27. A.C. Allori, A.M. Sailon, J.H. Pan, S.M. Warren, Biological basis of bone formation, remodeling, and repair-part III: biomechanical forces. Tissue Eng. Part B Rev. **14**, 285–293 (2008). https://doi.org/10.1089/ten.teb.2008.0084
28. D.J. Kelly, C.R. Jacobs, The role of mechanical signals in regulating chondrogenesis and osteogenesis of mesenchymal stem cells. Birth Defects Res. Part C Embryo Today **90**, 75–85 (2010). https://doi.org/10.1002/bdrc.20173
29. S. Judex, S. Gupta, C. Rubin, Regulation of mechanical signals in bone. Orthod. Craniofac. Res. **12**, 94–104 (2009). https://doi.org/10.1111/j.1601-6343.2009.01442.x
30. C. Alexandre, L. Vico, Pathophysiology of bone loss in disuse osteoporosis. Jt. Bone Spine **78**, 572–576 (2011). https://doi.org/10.1016/j.jbspin.2011.04.007
31. D.D. Bikle, T. Sakata, B.P. Halloran, The impact of skeletal unloading on bone formation. Gravit. Space Biol. Bull. **16**, 45–54 (2003)
32. G. Carmeliet, R. Bouillon, The effect of microgravity on morphology and gene expression of osteoblasts in vitro. FASEB J. **13** (Suppl), S129–S134 (1999)
33. K. Ziambaras, R. Civitelli, S.S. Papavasiliou, Weightlessness and skeleton homeostasis. Hormones **4**, 18–27 (2005)
34. R. Tamma et al. Microgravity during spaceflight directly affects in vitro osteoclastogenesis and bone resorption. FASEB J. **23**, 2549–2554 (2009). https://doi.org/10.1096/fj.08-127951
35. L. Benetatos et al. The microRNAs within the DLK1-DIO3 genomic region: involvement in disease pathogenesis. Cell. Mol. Life Sci. **70**, 795–814 (2013). https://doi.org/10.1007/s00018-012-1080-8
36. M. Stadtfeld et al. Aberrant silencing of imprinted genes on chromosome 12qF1 in mouse induced pluripotent stem cells. Nature **465**, 175–181 (2010). https://doi.org/10.1038/nature09017
37. L. He et al. A microRNA polycistron as a potential human oncogene. Nature **435**, 828–833 (2005). https://doi.org/10.1038/nature03552
38. K.A. O'Donnell, E.A. Wentzel, K.I. Zeller, C.V. Dang, J.T. Mendell, c-Myc-regulated microRNAs modulate E2F1 expression. Nature **435**, 839–843 (2005). https://doi.org/10.1038/nature03677
39. A.V. Olaru et al. MicroRNA down-regulated in human cholangiocarcinoma control cell cycle through multiple targets involved in the G1/S checkpoint. Hepatology **54**, 2089–2098 (2011). https://doi.org/10.1002/hep.24591
40. L. Lim et al. MicroRNA-494 within an oncogenic microRNA megacluster regulates G1/S transition in liver tumorigenesis through suppression of mutated in colorectal cancer. Hepatology **59**, 202–215 (2014). https://doi.org/10.1002/hep.26662
41. Romano, G. et al. MiR-494 is regulated by ERK1/2 and modulates TRAIL-induced apoptosis in non-small-cell lung cancer through BIM down-regulation. Proc. Natl Acad. Sci. USA **109**, 16570–16575, https://doi.org/10.1073/pnas.1207917109 (2012).
42. L. Li et al. Down-regulation of microRNA-494 via loss of SMAD4 increases FOXM1 and beta-catenin signaling in pancreatic ductal adenocarcinoma cells. Gastroenterology **147**, 485–497 e418 (2014). https://doi.org/10.1053/j.gastro.2014.04.048
43. H. Ohdaira, M. Sekiguchi, K. Miyata, K. Yoshida, MicroRNA-494 suppresses cell proliferation and induces senescence in A549 lung cancer cells. Cell Prolif. **45**, 32–38 (2012). https://doi.org/10.1111/j.1365-2184.2011.00798.x
44. S. Greco et al. Common micro-RNA signature in skeletal muscle damage and regeneration induced by Duchenne muscular dystrophy and acute ischemia. FASEB J. **23**, 3335–3346 (2009). https://doi.org/10.1096/fj.08-128579